Science of the Total Environment 635 (2018) 901–912

Contents lists available at ScienceDirect

Science of the Total Environment

journal homepage: www.elsevier.com/locate/scitotenv

An estimate of human and natural contributions to changes in water resources in the upper reaches of the Minjiang River

Jingwen Hou [a], Aizhong Ye [a,*], Jinjun You [b], Feng Ma [a], Qingyun Duan [a]

[a] State Key Laboratory of Earth Surface and Ecological Resources, Institute of Land Surface System and Sustainable Development, Faculty of Geographical Science, Beijing Normal University, Beijing 100875, China
[b] State Key Laboratory of Simulation and Regulation of Water Cycle in River Basin, China Institute of Water Resources and Hydropower Research, Beijing 100038, China

HIGHLIGHTS

- Water resources in the upper reaches of the Mingjiang River (UMR) basin decreased.
- Climate change had led to an increase in water resource availability in the UMR basin.
- Human activity had led to a decrease in water resource availability in the UMR basin.
- Multi-models can decrease the uncertainty of results.

GRAPHICAL ABSTRACT

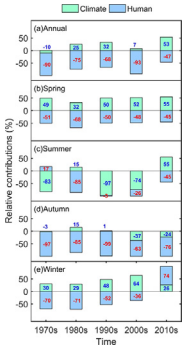

ARTICLE INFO

Article history:
Received 1 October 2017
Received in revised form 11 April 2018
Accepted 11 April 2018
Available online xxxx

Editor: D. Barcelo

Keywords:
Climate change
Human activities
Relative contribution
Water resources
Minjiang River basin

ABSTRACT

Climate change and human activities have changed the spatial-temporal distribution of water resources, especially in a fragile ecological area such as the upper reaches of the Minjiang River (UMR) basin, where they have had a more profound effect. The average of double-mass curve (DMC) and Distributed Time-Variant Gain Hydrological Model (DTVGM) are applied to distinguish between the impacts of climate change and human activities on water resources in this paper. Results indicated that water resources decreased over nearly 50 years in the UMR. At the annual scale, contributions of human activities and climate change to changes in discharge were −77% and 23%, respectively. In general, human activities decreased the availability of water resources, whereas climate change increased the availability of water resources. However, the impacts of human activities and climate change on water resources availability were distinctly different on annual versus seasonal scales, and they showed more inconsistency in summer and autumn. The main causes of decreasing water resources are reservoir regulation, and water use increases due to population growth. The results of this study can provide support for water resource management and sustainable development in the UMR basin.

1. Introduction

The hydrological cycle of watersheds in both spatial and temporal changes is a complex process that is widely influenced by climate change and human activities (Milliman et al., 2008; Zhang et al., 2011a; Song et al., 2013). The Intergovernmental Panel on Climate

* Corresponding author.
E-mail address: azye@bnu.edu.cn. (A. Ye).

https://doi.org/10.1016/j.scitotenv.2018.04.163
0048-9697/

Change (IPCC) report indicated that climate change has led to changes in global precipitation patterns since the 20th century, which has changed the global hydrological process and directly affect the spatial and temporal distribution of global water sources; thus, it can cause changes in discharge (Milly et al., 2005; Huntington, 2006). Human activities, such as changes in land use/cover, dam construction, and urbanization, have an obvious impact on all aspects of the water cycle (Sterling et al., 2013), which can greatly change the spatiotemporal distribution of water resources. The contradiction between the supply and demand of global water resources is becoming more and more prominent, primarily due to human activities and climate change (e.g., rapid economic development, increasing population and frequent extreme weather problems) (Wang et al., 2013; Luo et al., 2015a), which directly results in the reduction of discharge and causes challenges for global river ecosystem. Hence, it is of great significance to quantitatively assess the impact of climate change and human activities on discharge variations, which will enhance our understanding of the water cycle at both regional and global scales, improve water resource planning and management, and help to mitigate extreme weather events.

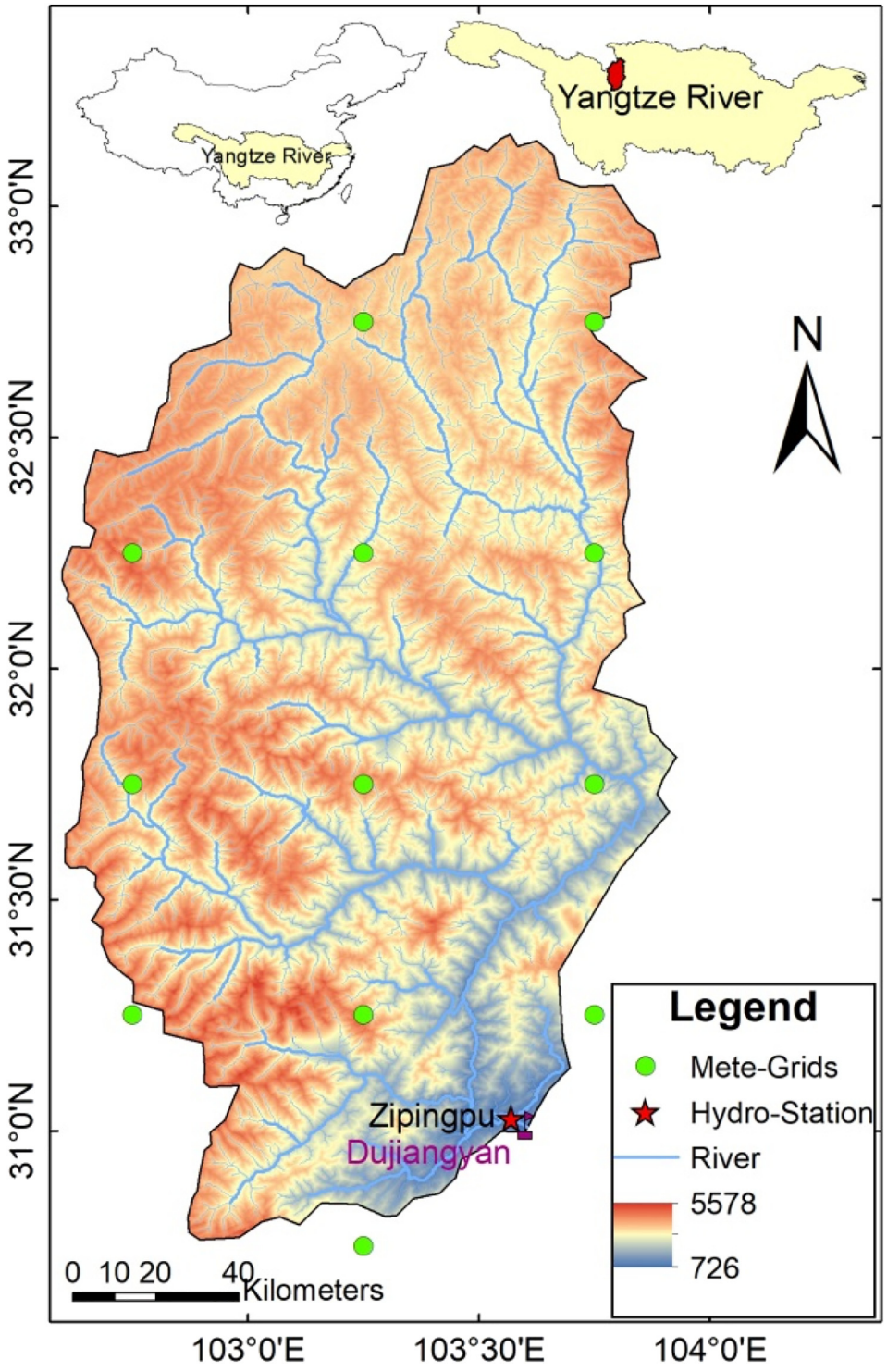

Fig. 1. Locations of the upper reaches of the Minjiang River Basin, meteorological grid points and hydrological station.

Numerous studies have demonstrated how to quantify the effects of climate change and human activities on discharge changes (Li et al., 2013; Zhang et al., 2016; Li et al., 2017). At present, three methods have already been applied: statistical analysis, elasticity methods and hydrological modeling. Wei and Zhang (2010)) used modified double-mass curves to determine the quantitative allocation of forest disturbance and climate variability to streamflow in the Willow River watershed. Yuan et al. (2016) used sensitivity analysis based on Budyko-type equations to indicate that climate change was the main driving factor controlling streamflow changes during the change period I (1981–2002), accounting for 60.07%–67.27% of the changes in most parts of Dongting Lake. However, human activity was the dominant factor during the change period II (2003—2010), accounting for 58.89%–78.33% of the changes. Li et al. (2016) employed the Soil and Water Assessment Tool (SWAT) model to separate out the effects of climate change, land cover change and direct human activities on the runoff variations in the Wei River Basin. Zhao et al. (2014) used Budyko's curve and linear regression methods to assess the potential impact of climate change and human activities on the annual mean streamflow in the middle reaches of the Yellow River basin (MRYRB). These results showed that human activities were the main driving factor in some tributaries, particularly in the northern basin. Li et al. (2017) utilized the Budyko framework and the hydrological model (SIMHYD) to study possible causes of the reduced discharge in the Yellow River basin. It was found that human activities were the main reason for the decrease in discharge, and it reduced discharge by 73.4% and 82.5% in 1980–2000 and 2001–2014, respectively.

The Minjiang River is the largest tributary in the upper reaches of the Yangtze River. Many studies of the Minjiang River have analyzed the trends and variable characteristics of water resources. Yang et al. (2014) analyzed and predicted the tendency of precipitation and runoff from 1955 to 2008 at the UMR. The result indicated that both precipitation and runoff had decreasing trends and that changes in runoff had a certain lag relative to changes in precipitation. Zhang et al. (2012) used a combination of statistical analysis and graphical methods to obtain the relative contributions of climate variability and forest disturbance to annual runoff, and they clearly showed that forest harvest and climate change had an offsetting effect on annual runoff changes. While it is meaningful to study the contribution of forest disturbance to runoff changes, it does not fully represent all human activities. After all, human activities include many factors. In recent years, elasticity methods have been widely applied to separate the contributions of climate change and human activities on discharge changes at different spatial scales. Wang (2014) showed that elasticity methods do not eliminate the impact of human activities on the baseline periods, resulting in a bias in the contribution rate. In addition, elasticity methods are based on an annual time scale, which is rough and cannot be used to quantitatively analyze the impact of climate change and human activities on discharge variations during the year (Hu et al., 2012). Therefore, we choose a combination of statistical analysis (DMC) and hydrological modeling (DTVGM) to analyze the contribution of human activities and climate change to discharge changes in the UMR.

The objectives of this study are as follows: (1) to determine the change trend of precipitation on a spatiotemporal scale in the UMR and compare them with the variation tendency of discharge at Zipingpu station (the outlet of the upper reaches of the Minjiang River) from 1961 to 2012; (2) to compare the difference and consistency of the double-mass curve (DMC) and Distributed Time-Variant Gain Model (DTVGM) in assessing the effects of climate change and human activities to discharge changes on different time scales; (3) to quantify and compare the relative contributions of climate change and human activities to discharge changes on annual and seasonal scales; (4) to discuss the possible causes of discharge variations due to climate change and human activities.

This paper is organized as follows: Section 2 introduces the study area and data; Section 3 describes the methodologies, including the Mann-Kendall test, the Double-mass curve method (DMC), the Distributed Time-Variant Gain Model (DTVGM) and the Quantitative estimate method; Section 4 presents the results and discussion; and Section 5 presents the conclusions.

2. Study area and data

2.1. Study area

The Minjiang River is an important tributary of the Yangtze River (Fig. 1). The upper reaches of the Minjiang River (UMR) refers to the river above Dujiangyan, which is the main source of water for agriculture, industry and life in the Chengdu Plain. The ecological environment of the UMR is very vulnerable because of its typical alpine gorge landscape, which mainly comprised the following: the sharp decline in forest area, severe soil erosion and frequent natural disasters. In recent years, the discharge of the Minjiang River has continued to decrease, and making the contradiction between the supply and demand of water resources more prominent. Thus, it is necessary to better understand these hydrological processes, then, to quantify the contribution of human activities and climate change to discharge variations in the UMR. The UMR has a drainage area of 22,722 km^2 and ranges in elevation from 726 m to 5578 m. The Dujiangyan was constructed around 256 BCE by the State of Qin as an irrigation and flood control project, and it is still in use today.

The precipitation in the UMR basin has a strong seasonality, with >60% of the annual precipitation (987 mm, 1961–2012) concentrated in the flood season from May to September, which is caused by the typical continental monsoon climate and is characterized by long-lasting and light intensity (Fig. 2). The annual mean discharge is 462 m^3/s, and the annual mean water resource availability is 14.5 billion m^3 at Zipingpu station. The runoff coefficient describes the ability to produce runoff in the basin, and it is affected by the underlying condition. Fig. 2 shows that the runoff coefficients are <1 in the UMR basin, except in November, December and January. Runoff coefficients >1 may be caused by the fact that runoff comes from alpine snowmelt, soil water and reservoir outflow in winter. The runoff coefficients in the UMR basin show the periodicity change rule during the study period, and it reaches its peaks in January and December.

2.2. Data

Daily precipitation data during 1961–2012 was collected from the China Meteorological Administration (CMA), with a spatial scale of a 0.5-degree grid (Table 1). The daily discharge data of the Zipingpu

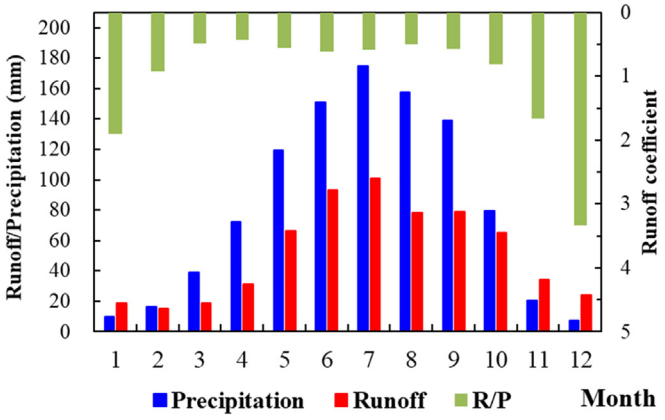

Fig. 2. The mean seasonal cycle of precipitation, runoff and runoff coefficient (R/P: runoff/precipitation) in the upper reaches of the Minjiang River Basin (1961–2012).

Table 1
Information of base data in the upper reaches of the Minjiang River Basin.

Data types	Scale	Source	Data attributes
DEM	3 s	USGS	Elevation
Precipitation	0.5°	CMA http://data.cma.cn/	Daily and monthly precipitation during 1961–2012
Discharge	Zipingpu station	Hydrological yearbook	Daily discharge during 1961–2012, annual discharge during 1937–2012

hydrological station was gathered from the Hydrological Yearbook of the China Hydrological Bureau. The DEM data was obtained from the NASA Shuttle Radar Topography Mission (SRTM) 3 arc-seconds digital elevation data. Population data from 1964 to 2010 was obtained from the Sichuan Statistical Yearbook. The data of the cumulative numbers of reservoirs in the UMR was taken from Li (2014). There are 187 reservoirs, 4 large hydropower stations and 29 middle hydropower stations in the UMR by 2017. The total reservoir storage is >20 billion m^3. Land use data were collected from Li et al. (2005) and Tan (2016) for 1972, 1986, 1990, 2000, 2010, and 2015. The grassland area is about 50% and forest land area is about 46% in the UMR, and the other land use distribution is <5%.

3. Methodologies

The Mann-Kendall test method was used to detect the trend and mutation point of discharge. The double-mass curve method and the Distributed Time-Variant Gain Hydrological Model (DTVGM) were employed to quantify the influences of climate change and local human activities on discharge changes.

3.1. Mann-Kendall test

The Mann-Kendall test (M-K) is a nonparametric test used for trend and mutation detection in time series (Mann, 1945; Kendall, 1948). The Mann-Kendall test, as recommended by the World Meteorological Organization (WMO), is a nonparametric statistical method (Mitchell et al., 1966) widely used in the trend analysis and mutation detection of hydro-meteorological data. For a time-series of n observations, $X = x_1, x_2, \ldots, x_n$, the M-K trend statistic (S) is computed using Eq. (1) and Eq. (2). In this study, the autocorrelation of the data did not reach a significant threshold of 0.05; thus, we directly used raw data to perform the Mann-Kendall trend analysis (Yue et al., 2002; GAO et al., 2010).

$$S = \sum_{i=1}^{n-1} \sum_{j=i+1}^{n} sign\,(x_j - x_i) \tag{1}$$

$$sign\,(x_j - x_i) = \begin{cases} 1, & x_j > x_i \\ 0, & x_j = x_i \\ -1, & x_j < x_i \end{cases} \tag{2}$$

If the sample size n is large enough ($n > 10$), the standard normal variable Z can be used to evaluate the trend of the time-series (Eq. (3) and Eq. (4)). $E(S)$ and $\mathrm{Var}(S)$ are the expected value and variance of S, respectively. This time-series has increasing trends if the value of Z is greater than zero; otherwise, the time-series has decreasing trends. If $|Z| \geq Z_{1-(\alpha/2)}$, the null hypothesis of no trend is rejected at the significance level α. The null hypothesis can be tested at 5% and 10% significance levels. The values of $Z_{1-(\alpha/2)}$ at the 5% and 10% significance levels are 1.96 and 1.28, respectively.

$$Z = \begin{cases} \dfrac{S-1}{\sqrt{Var\,(S)}}, & S>0 \\ 0, & S = 0 \\ \dfrac{S+1}{\sqrt{Var\,(S)}}, & S<0 \end{cases} \tag{3}$$

$$E(S) = 0 \quad Var\,(S) = \frac{n\,(n-1)\,(2n+5)}{18} \tag{4}$$

For a time-series of n observations $X = x_1, x_2, \ldots, x_n$, the M-K mutation statistic (S_j) is computed using Eq. (5) and Eq. (6).

$$S_1 = 0, \quad S_j = \sum_{i=1}^{j} r_i, \quad (j = 2, 3, \cdots, n) \tag{5}$$

$$r_i = \begin{cases} 1, & x_i > x_j \\ 0, & x_i \leq x_j \end{cases} \tag{6}$$

The standard normal distribution UF_j can be calculated based on the X series (Eq. (7) and Eq. (8)). (S_j) and $\mathrm{Var}(S_j)$ are the expected value and the variance of S_j, respectively. If $|UF_j| > U_\alpha$, the hypothesis of the trend is accepted at the significance level α. The time-series has increasing trends if the value of UF_j is greater than zero; otherwise, the time-series has decreasing trends.

$$UF_1 = 0 \quad UF_j = \frac{S_j - E(S_j)}{\sqrt{\mathrm{var}(S_j)}}, \quad (j = 2, 3, \cdots, n) \tag{7}$$

$$E(s_j) = \frac{n(n+1)}{4} \quad Var(s_j) = \frac{n(n-1)(2n+5)}{72} \tag{8}$$

Table 2
Description of the common verification measures used in the study. The x is observed data, y is simulated data, i is time, and N is the total number of data.

Verification measures	Formulas	Descriptions	Perfect/no skill
Nash-Sutcliffe efficiency value (NSE)	$\mathrm{NSE} = 1 - \frac{\sum_{i=1}^{N}(x_i - y_i)^2}{\sum_{i=1}^{N}(y_i - \bar{y})^2}$	Assessing the predictive power of hydrological models; quantitatively describe the accuracy between forecasts and observations	1/≤0
NSE calculated on inverse transformed flows	$\mathrm{NSE}_I = 1 - \frac{\sum_{i=1}^{N}(\frac{1}{x_i} - \frac{1}{y_i})^2}{\sum_{i=1}^{N}(\frac{1}{y_i} - \overline{\frac{1}{y_i}})^2}$		
Root mean square error (RMSE)	$RMSE = \sqrt{\frac{1}{N}\sum_{i=1}^{N}(x_i - y_i)^2}$	Association of forecasts and observations over a long time period	0/∞
Pearson correlation coefficient	$R = \frac{\sum_{i=1}^{N}(x_i - \bar{x})(y_i - \bar{y})}{\sqrt{\sum_{i=1}^{N}(x_i - \bar{x})^2}\sqrt{\sum_{i=1}^{N}(y_i - \bar{y})^2}}$	Linear dependency between forecasts and observations	1/≤0
Relative bias	$rBias = (\sum_{i=1}^{N} x_i \Big/ \sum_{i=1}^{N} y_i - 1) \cdot 100\%$	Relative difference between forecasts and observations	0/∞

The standard normal distribution UB_j can be calculated based on the reversed order of the X series using the same method. The intersection point of the UF and UB curves reflects the beginning of the abrupt change (Zhang et al., 2011b).

3.2. Double-mass curve method

The double-mass curve (DMC) method has been proven to be a relatively simple and effective statistical method that is used to study the consistency of long-term hydro-meteorological data (Mu et al., 2010). When the DMC method is used to extrapolate, there is a hypothesis that the background before and after abrupt point is consistent (Gao et al., 2010). The relationship between cumulative observed precipitation ($CP_j^{bas} = \sum_{i=1}^{j} P_i^{bas}$, P is precipitation) and cumulative observed discharge ($CD_j^{bas} = \sum_{i=1}^{j} D_i^{bas}$, D is discharge) during the baseline period can be expressed as:

$$CD_j^{bas} = a \cdot CP_j^{bas} + b, \quad (j = 1, 2, \cdots, n) \tag{9}$$

where n represents the length of the time series, j is the number of years, a is a correction or rate of change, and b donates the intercept.

According to the linear regression equation established in the baseline period (Eq. 9), the cumulative simulated discharge ($CD_j^{sim} = \sum_{i=1}^{j} D_i^{sim}$) of the changed period can be obtained using the cumulative observed precipitation ($CP_j^{var} = \sum_{i=1}^{j} P_i^{var}$) during the period of change. Finally, the annual simulated discharge D_j^{sim} can be calculated based on two years of cumulative simulated discharge. The specific formula is as follows:

$$CD_j^{sim} = a \cdot CP_j^{var} + b, \quad (j = 1, 2, \cdots, n) \tag{10}$$

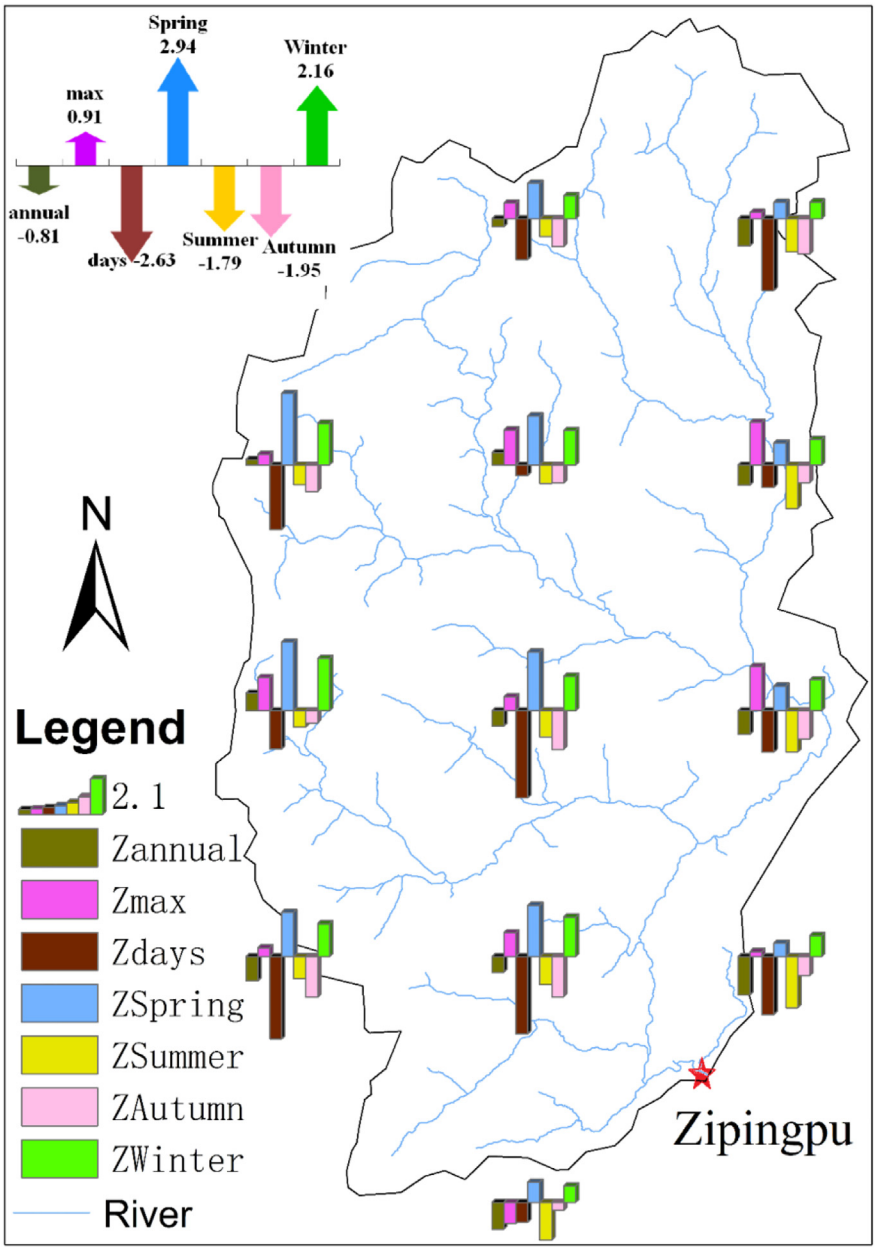

Fig. 3. M-K test values of precipitation in the Upper reaches of the Minjiang River basin (1961–2012). "Zannual" is the Z-value of the annual precipitation; "Zdays" is the Z-value of wet days (daily precipitation >1 mm); "Zmax" is the Z-value of the annual maximum daily precipitation. "Spring" is March to May. "Summer" is June to August. "Autumn" is September to November. "Winter" is December to next February.

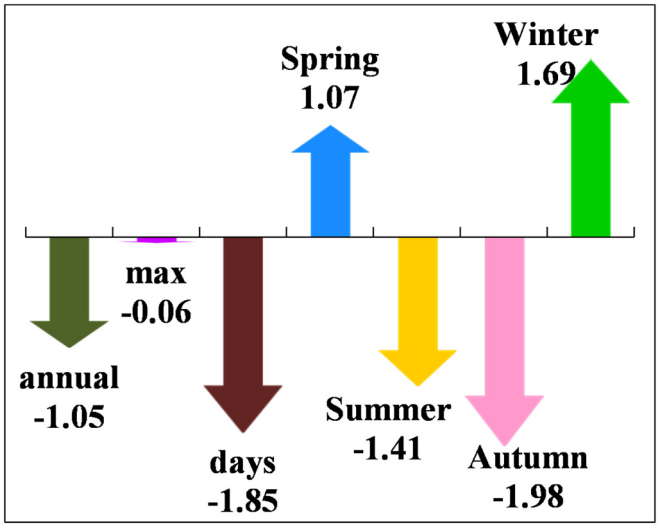

Fig. 4. M-K test values of observed discharge in the Upper reaches of the Minjiang River basin (1961–2012). "annual" is the Z-value of the annual mean discharge, "max" is the Z-value of the annual maximum daily discharge, "days" is the Z-value of flood days (daily discharge > 1055 m^3/s), "Spring" is the Z-value of the March to May mean discharge, "Summer" is the Z-value of the June to August mean discharge, "Autumn" is the Z-value of the September to November mean discharge, and "Winter" is the Z-value of the December to next February mean discharge.

$$D_j^{sim} = CD_j^{sim} - CD_{j-1}^{sim}, \quad (j = 1, 2, \cdots, n) \tag{11}$$

3.3. Distributed hydrological model

The Distributed Time-Variant Gain Hydrological Model (DTVGM) was proposed by Xia et al. (2003), and has been applied to several basins (Wang et al., 2002). The runoff module is a simple nonlinear time-variant gain hydrological model (TVGM), and the effectiveness of the TVGM in rainfall-runoff simulations is better than that of linear models (Xia, 1991). The DTVGM is a water balance model that uses sub-basins (Ye et al., 2010). Eq. (12) shows the water balance equation for a sub-basin:

$$P = \Delta W + g_1 \left(\frac{W_u}{WM_u \cdot C}\right)^{g_2} \cdot P + K_r \cdot W_u + f_c \cdot \left(\frac{W_g}{WM_g}\right)^{K_g} + Ep \cdot \left(\frac{W_u}{WM_u \cdot C}\right) \tag{12}$$

where P is precipitation (mm); ΔW is the change in soil moisture (mm); W_u is the upper soil moisture at the sub-basin (mm); W_g is the lower soil moisture at the sub-basin (mm); WM_u is the upper field soil moisture (mm); u is the "upper" soil; WM_g is the lower field soil moisture (mm); f_c is the soil permeability coefficient (mm/h); g_1 and g_2 are parameters ($0 < g_1 < 1{,}0 < g_2$); g_1 is the runoff coefficient when the soil is saturated; g_2 is the soil moisture parameter; C is the land cover parameter; K_r is the sub-surface runoff coefficient; and K_g is the groundwater runoff coefficient.

The kinematic wave model is used for routing analysis (Ye et al., 2006; Ye et al., 2013). The DTVGM assumes that the river flow is gradually varying unsteady flow in open channels. Eq. (13) shows the continuity equation:

$$\frac{\partial A}{\partial t} + \frac{\partial Q}{\partial x} = q \tag{13}$$

where A is the river cross section area (m^2); t is time (s); Q is discharge (m^3/s); x is the flow path (m), and q is the lateral inflow (m^2/s).

3.4. Estimating the contributions of climate change and human activities to discharge

In order to quantitatively assess the contributions of climate change and human activities to discharge changes, the entire study period was divided into two parts: a baseline (benchmark) period (Zhang et al., 2016), and a changed period (Chang et al., 2016). The discharge changes in the baseline period are mainly due to climate change, while the discharge changes in the changed period result from both climate change and human activities (Eq. (14)):

$$\Delta Q_t = \Delta Q_c + \Delta Q_h = Q_{obs} - Q_{base} \tag{14}$$

where ΔQ_t is the total discharge changes, ΔQ_c is the discharge change due to climate change, and ΔQ_h is the discharge change due to human activities. Q_{obs} represents the observed discharge during the changed period, and Q_{base} represents the average observed discharge during the baseline period.

The simulated discharge (Q_{sim}) was obtained from the hydrological model or the cumulative precipitation-discharge regression model, which is calibrated based on the observed discharge during the benchmark period. The impact of new human activities (e.g. reservoirs, irrigation and afforestation) can seldom be simulated by models, so we used the difference between Q_{obs} and Q_{sim} as the discharge change due to new human activities during the changed period (Eq. (15)), and the difference between Q_{sim} and Q_{base} reflected the change in discharge due to climate change (Eq. (16)).

$$\Delta Q_h = Q_{obs} - Q_{sim} \tag{15}$$

$$\Delta Q_C = Q_{sim} - Q_{base} \tag{16}$$

The relative contributions of climate change (η_c) and human activities (η_h) to discharge changes can be calculated using Eq. (17) (Ma et al., 2014; He et al., 2013). The discharge increases if η is greater than zero, otherwise, the discharge decreases.

$$\eta_h = \frac{\Delta Q_h}{|\Delta Q_c| + |\Delta Q_h|} \cdot 100\% \quad \eta_c = \frac{\Delta Q_c}{|\Delta Q_c| + |\Delta Q_h|} \cdot 100\% \tag{17}$$

3.5. Model performance measures

The model performance measures include the Nash-Sutcliffe efficiency (*NSE*) value, the correlation coefficient *R*, the Root Mean Square Error (RMSE), and the Relative Bias (*rBias*), which are computed in Table 2.

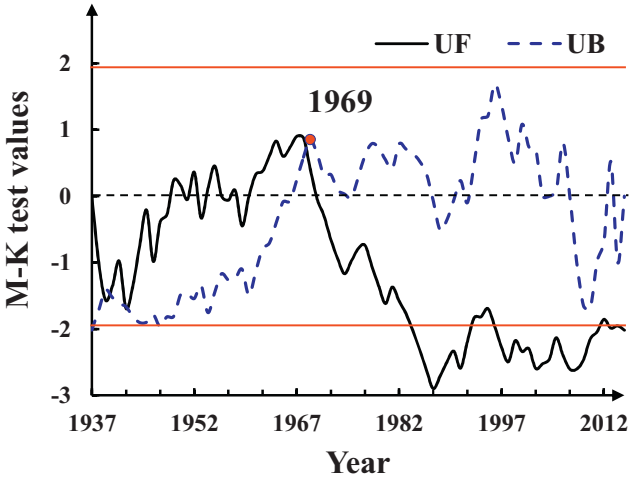

Fig. 5. M-K mutation analysis of annual discharge at Zipingpu station during 1937–2012.

4. Results and discussion

4.1. Trend analysis of precipitation and discharge

The Mann-Kendall test values of precipitation across time and space during 1961–2012 are shown in Fig. 3. Trend analysis indicates that the *Z*-value of annual precipitation in the UMR is −0.81, which does not reach the significant threshold of 0.05 and only shows a non-significant downtrend. In terms of spatial distribution, the annual precipitation shows a downward trend except the north-western region in the UMR basin. From the trend of seasonal changes in the whole study area, the precipitation in spring (ZSpring = 2.94) and winter (ZWinter = 2.16) both have prominent increasing trends at the 0.05 significance level. The trends are opposite in the summer and autumn, but only display a slight decline in the summer (ZSummer = −1.79) and autumn (ZAutumn = −1.95). The trends of precipitation at each grid point are consistent with the trends of the entire study area on different seasonal scales, although the Z values are different. Annual maximum daily precipitation increases, and wet days (the daily precipitation is >1 mm) decrease, which means the precipitation is heavy and concentrated. Thus, it is of great significance for the management of water resources to understand the spatial and temporal distributions of water resources throughout the year.

The Mann-Kendall test was used to detect the change trends of annual and seasonal discharge at Zipingpu station. The discharge changes are shown in Fig. 4. The M-K test index Z is −1.05 for the annual discharge, which indicates that no significant decreasing trend occurred from 1961 to 2012. The maximum daily discharge and the flood days (with a daily discharge >1055 m^3/s, 5% frequency flood) also show no significant decreasing trends. However, the changing trend of the annual maximum daily discharge is opposite that of the annual maximum daily precipitation, which indicates that the underlying surface condition has a great influence on the direction of the discharge changes. The average seasonal discharge increases in spring and winter and decreases in summer and autumn. These phenomena are mainly due to precipitation changes, and show good consistency with precipitation variations on seasonal and annual scales (Fig.3).

4.2. Mutation analysis of observed discharge

The annual discharge trend analysis of Zipingpu station is shown in Fig. 5. The black line indicates the UF value, and the blue dotted line represents the UB value. The red line is 1.96 (−1.96) of the 5% significance level. The intersection of the curves reflects an abrupt change in the annual discharge that occurred in 1969. Based on the M-K test, the period of the discharge record was divided into two parts: a baseline period (1961–1969) representing discharge under natural conditions, and a changed period (1970–2012) representing discharge under the combined influence of human activities and natural conditions.

Table 3
Performance indices calculated for discharge simulations at Zipingpu station.

	Calibration period, daily (1961–1965)	Verification period, daily (1966–1969)
NSE	0.73	0.72
R	0.87	0.85
NSE_I	0.43	0.77
RMSE	177	185
rBias	4.2%	2.1%

4.3. Model calibration and performance assessment

The baseline period (1961–1969) was divided into two parts: a calibration period (1961–1965) and a verification period (1966–1969) (Fig. 6). The distributed hydrological model took a long time to run, and automatic calibration would be too time-consuming, so we used a manual calibration method to calibrate the model parameters. The model was run a few times to ensure that *NSE* (NSE_I), *R* and *rBias* were good during manual calibration.

The NSE values are 0.73 and 0.72 between the simulated discharge and observed discharge during the calibration and verification periods, respectively (Table 3). The correlation coefficient R is >0.85, and the Relative Bias is 4.2% for the calibration period. The NSE_I (Pushpalatha et al., 2012) was used to verify the low flow simulation. These results demonstrate that the hydrological model has sufficient accuracy for the long-term simulation of discharge without considering the influence of human activities. The NSE_I (0.43) value is low in calibration period which shows the model simulates low flows poorly. The main cause is low flow simulation can also be complicated by human activities that alter natural streamflow via reservoir regulation or water diversion for irrigation (Ye et al., 2015).

Fig. 6 and Fig. 7 show the simulated and observed discharge at Zipingpu station for the baseline period and changed period, respectively. The two figures show good agreement between the simulated and observed discharge. The relationship between discharge and precipitation is stable, which demonstrates that the DTVGM can be used to analyze the impacts of climate change and human activities on changes in water resources. The difference between the simulated and observed discharge represents the impact of human activities on water resources change during the changed period.

Fig. 8 presents the double-mass curves for the cumulative discharge and cumulative precipitation from 1961 to 2012 on different time scales. The correlation coefficients (R^2) are all >0.99, thus showing a high degree of correlation. In other words, the DMC method is reliable

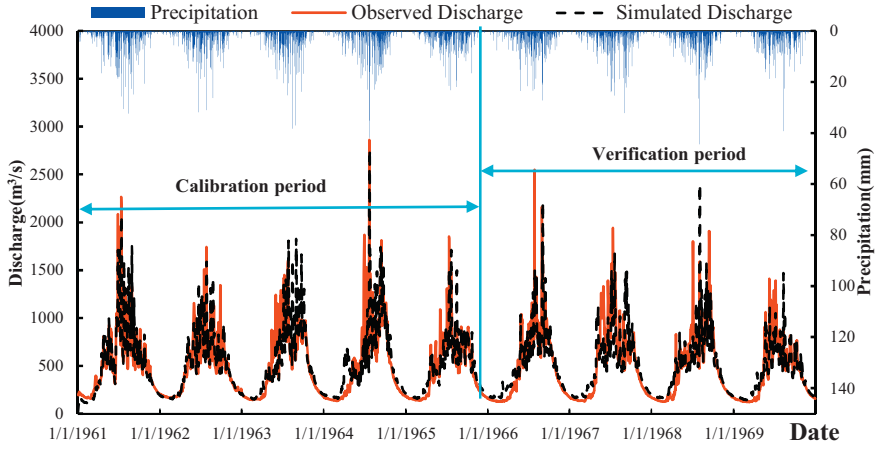

Fig. 6. Long-term daily hydrographs for the calibration period (1961–1965) and the verification period (1966–1969) at Zipingpu station.

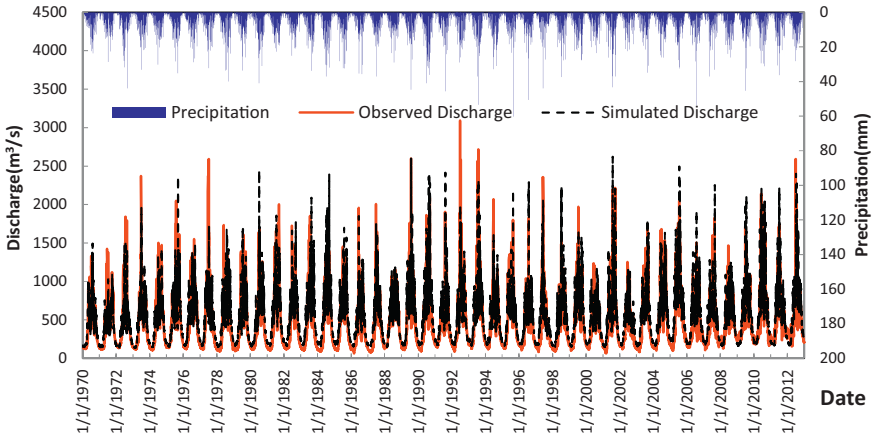

Fig. 7. Long-term daily hydrographs for the changed period (1970–2012) at Zipingpu station.

because the reconstruction equations perform well during the baseline period. The relationship between discharge and precipitation is not linear and stationary, caused by human activities. The cumulative observed discharge curves gradually drop below the red regression lines, thus indicating that human activities decrease the discharge. Although the impact of human activities on discharge is different in different seasons, it caused discharge to decrease in all seasons.

4.4. Quantitative evaluation of the impact of climate change and human activities on discharge variations

The contributions of climate change and human activities to discharge changes is separated using the DMC and DTVGM models in the changed period (1970–2012), as shown in Fig. 9, on annual and seasonal scales. The horizontal axis represents time and the vertical axis represents the discharge changes (m^3/s). It can be seen clearly from Fig. 9 that the patterns of discharge changes obtained using these two methods are overall very similar in distinguishing impacts on different temporal scales. Therefore, we can obtain more reliable results by combining the DMC and DTVGM methods. The histogram shown in Fig. 9 represents the average of the discharge changes based on these two methods. The magnitude and direction of the influence of climate change and human activities on discharge changes are different on annual and seasonal scales. Thus, it is necessary to study the response of water resources on both seasonal and annual scales, which is beneficial to the allocation of water resources within a year. In general, climate change tends to increase discharge and human activities tend to decrease discharge on different time scales, except during summer and autumn when the discharge changes caused by climate change and human activities do not have a specific rule.

Fig. 10 shows the relative contributions of climate change and human activities to discharge changes on annual and seasonal scales, calculated using the average discharge variations obtained by the DMC and DTVGM models. At the annual scale, human activities are the dominant factor affecting discharge changes, and tend to reduce discharge, accounting for −90%, −75%, −68%, −93% and − 47% in the 1970s, 1980s, 1990s, 2000s and 2010s, respectively. However, the impact of climate change on discharge variations trends to increase discharge apart from 1970s, accounting for −10%, 25%, 32%, 7%, and 53% in the 1970s, 1980s, 1990s, 2000s and 2010s, respectively. In general, the contributions of human activities and climate change to discharge changes were −77% and 23%, respectively. At seasonal scales, particularly in the spring and winter, the direction of the influence of climate change and human activities on discharge changes is basically consistent with the direction of the influence at the annual scale. Compared to human activities, climate change is the main driving factor of the discharge changes in the summer, yet, it has the opposite driving factor in autumn from the 1970s to 2010s. Determining the main causes of changes in water resources within the year is helpful in reducing flood and drought risks, especially vulnerable region like the UMR.

4.5. Discussion

Climate change, especially precipitation, is a key factor in discharge, which changes the magnitude and spatial distribution of precipitation. It can be seen from Fig. 3 that the annual precipitation presents a slight decreasing trend, and the annual discharge corresponds well to annual precipitation (Fig. 4) in the UMR from 1961 to 2012. On a seasonal scale, seasonal precipitation and discharge have synchronized changes. This means that precipitation directly influences discharge variations.

As shown in Fig. 11a, the trends of precipitation changes and discharge changes were opposite in the 1970s–1990s and consistent in the 1990s–2010s at the annual scale. Except during the 2000s, the annual precipitation changes relative to the baseline period are positive; however, the annual discharge changes are all negative, except during the 2010s. This reflects the combined effects of climate change and human activities. At seasonal scales (Fig. 11b-e), there was a good match between the trends of precipitation changes and discharge changes in spring and summer, although differences still exist in their specific magnitude. On the other hand, there was little correlation in autumn and winter months. These results indicate that human activities play an important role in changing the mechanism of precipitation-discharge, which directly affects discharge variations.

With societal development, human activities, changing the underlying surface to change the relationship between precipitation and discharge, have constantly intensified over the past 52 years. Human activities, such as population increase, water conservancy construction, and land use change, have altered natural water circulation patterns. Fig. 12 shows changes in population size, the cumulative number of reservoirs, and land use area in the UMR basin from 1961 to 2012. Fig. 12a illustrates that the population has grown over the past 52 years in the UMR basin. The total population size is not large, and growth was rapid before the 1990s and slow after the 1990s. This increase in population size is always accompanied by an increase in water consumption, which inevitably results in the reduction of discharge. Hydropower development started early and was constructed rapidly in the UMR, which resulted in the construction of 187 reservoirs by 2017 (Fig.12b). On the one hand, the reservoirs have a direct impact on discharge, such as seasonal water storage and diversion, it can be used to adjust the seasonal distribution of water resources and to prevent floods and droughts. This may be the main reason for the inconsistency of discharge and precipitation throughout the seasons. On the other hand, the cumulative effects of multilevel hydropower cannot be ignored, and we found that river dehydration occurred consistently in the UMR basin, which

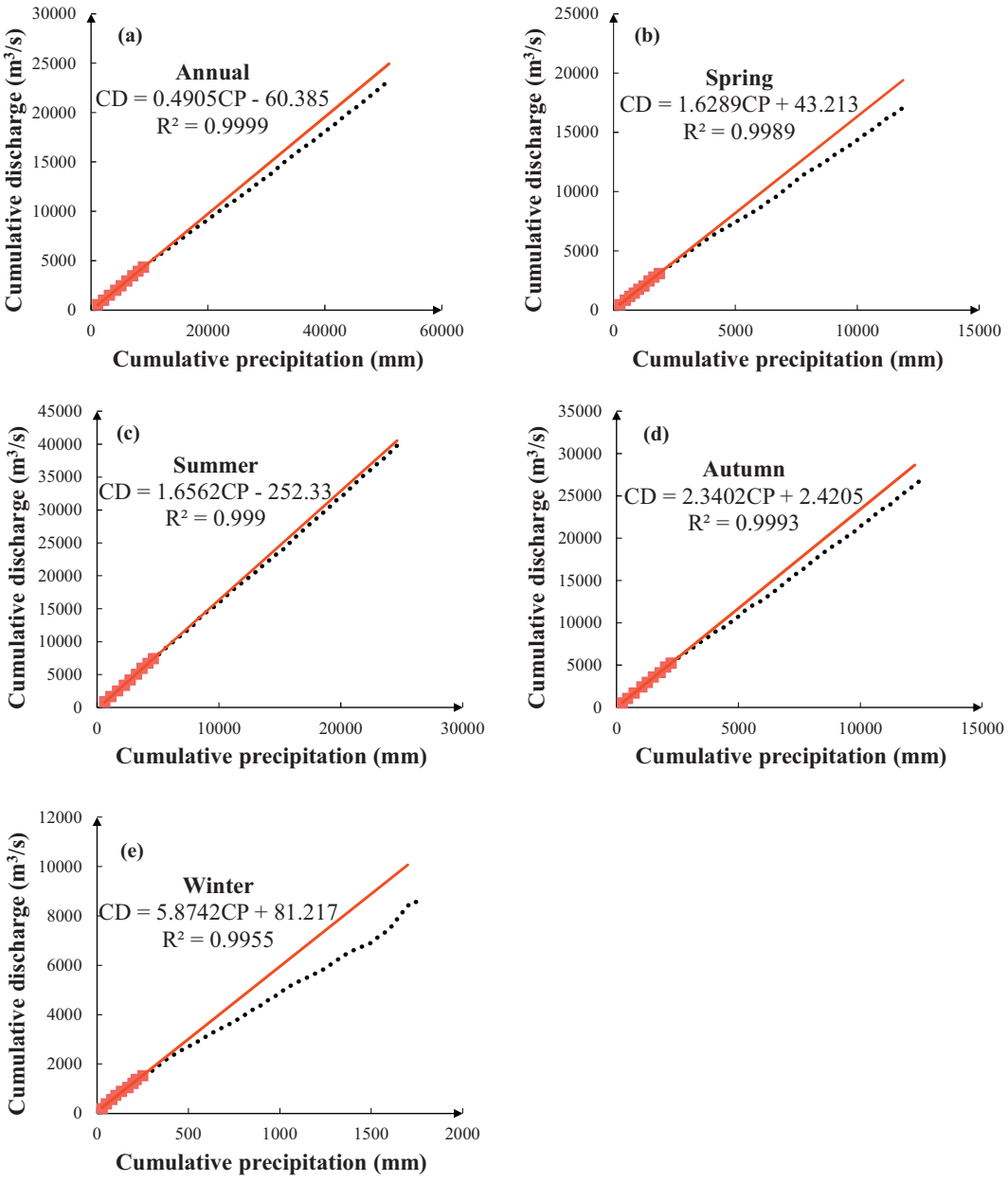

Fig. 8. Double-mass curves between cumulative discharge and cumulative precipitation from 1961 to 2012 in different seasons. The red lines represent the linear regression between the cumulative observed discharge and cumulative observed precipitation during the corresponding baseline period (1961–1969), and are extended to the post-baseline period to represent cumulative simulated discharge. The black dotted lines represent the relationship between cumulative observed precipitation and cumulative observed discharge during 1961–2012. (For interpretation of the references to colour in this figure legend, the reader is referred to the web version of this article.)

directly reduced the magnitude of discharge and changed the distribution of water resources.

Land use change can cause meaningful changes in hydrological processes (Fig. 12c-d). Luo et al. (2015b) explored the influence of land use change on hydrological processes by designing extreme rainfall over the period 1976 to 2006 in the Kamo River basin. The results showed that the discharge was different under different land use patterns. As Fig. 12c shows, the cultivated land area experienced growth overall, and increased rapidly in 1990–2010, reaching its maximum value of 731.87 km^2 by 2010. Afterwards, the area of cultivated land decreased to 699 km^2 in 2015. More cultivated land requires more irrigating water. The trends of forest area and grassland are just the opposite. During the early days of the People's Republic of China, the destruction of forests in the URM basin increased annually from 1950 to 1978 (Bao et al., 1995; Zhang, 1992). Additionally, the sharp decline in forest area is an important reason for the decrease of discharge in the URM (Fig. 11 and Fig. 12c). With reforestation, the forest began to recover, and its area reached 11,467.92 km^2 by 1990. After the flood of the Yangtze River in 1998, the UMR began to implement the Natural Forest Protection and the Grain-to-Green Program, and the forest area was further expanded in the UMR basin. Thus, it is necessary to control the area of the forest, and we cannot blindly add plants or cut them down. After all, the response of discharge to forest changes is prominent in the UMR basin (Zhang et al., 2012). Fig. 12d shows that the water area increased by 79.73 km^2 from 1972 to 2015, and the largest water area was 127.85 km^2 in 2010. Increased water area will cause an increase in actual evaporation, leading to reduced discharge. There is a clear increase in construction land area and unused land area in 2010. This may be related to the 2008 earthquake in Wenchuan. In addition, the 2008 Wenchuan earthquake caused forests to shrink from 2010 to 2015 and grasslands to expand. As the area of construction land increased, the amount of infiltration and vaporization decreased, which

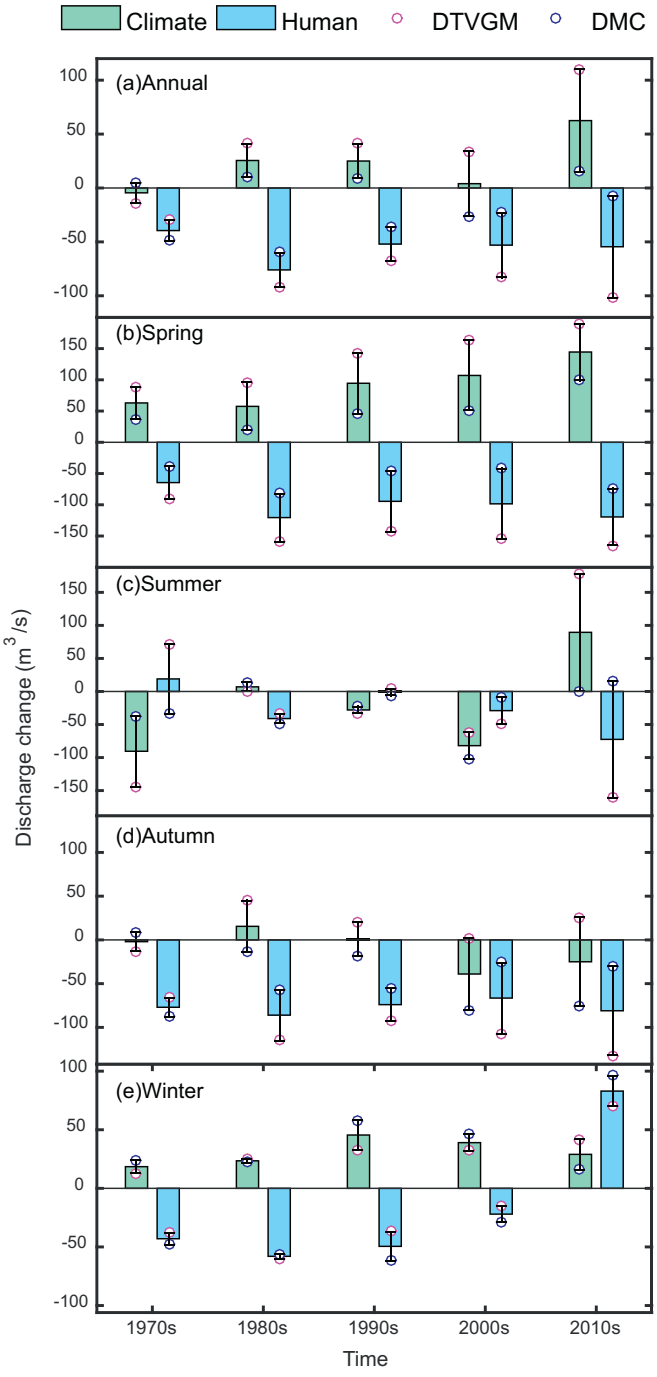

Fig. 9. Comparison of the contributions of climate change and human activities to discharge changes on annual and seasonal scales, calculated from the DMC and DTVGM models.

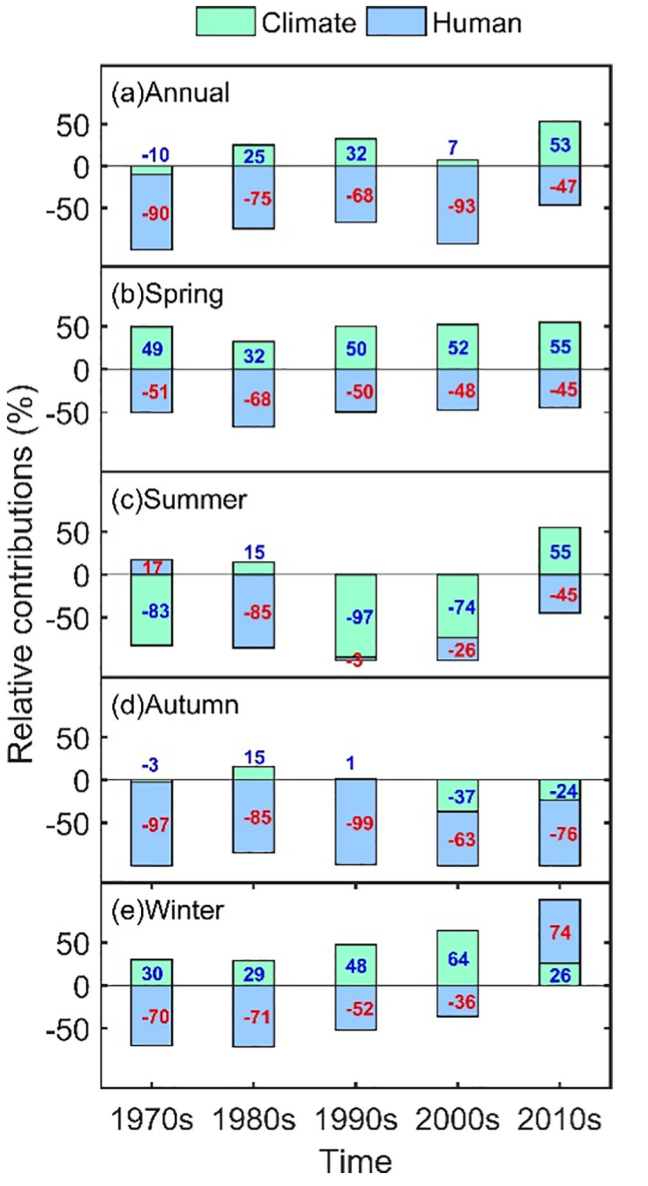

Fig. 10. Comparison of the relative contributions of climate change and human activities to discharge changes on annual and seasonal scales, calculated from the average of the DMC and DTVGM models.

leads to increased discharge. The discharge variation results from the combined effects of climate change and human activities, with many impact factors and complex changes.

5. Conclusions

The Minjiang River is an important tributary of the upper reaches of the Yangtze River; meanwhile, the UMR is the main water source in the Chengdu Plain, as a case study area, the purpose of this article is to quantify the relative contributions of climate change and human activities to discharge changes at annual and seasonal scales in the UMR, which is a vulnerable region, and to discuss the possible causes of discharge changes to support the decisions of relevant departments. The main conclusions of this study are as follows:

(1) The patterns of discharge changes, affected by climate change and human activities, obtained using the two methods are overall very similar at different temporal scales from 1970 to 2012. We use the average results of the DMC and DTVGM methods to assess the relative contributions of climate change and human activities to discharge changes in the UMR basin. Using these two methods to cross validate each other will make their results more reliable.

(2) In general, climate change contributed to an increase in water resources, and human activities played an important role in decreasing water resources in the UMR. Human activities were the major driving factor of discharge changes at the decadal scale, and tended to reduce discharge, accounting for −90%, −75%, −68%, −93% and −47% in the 1970s, 1980s, 1990s, 2000s and 2010s, respectively. Relative contributions displayed similar change directions on spring, winter and decadal scales, but there were more inconsistent during summer and autumn.

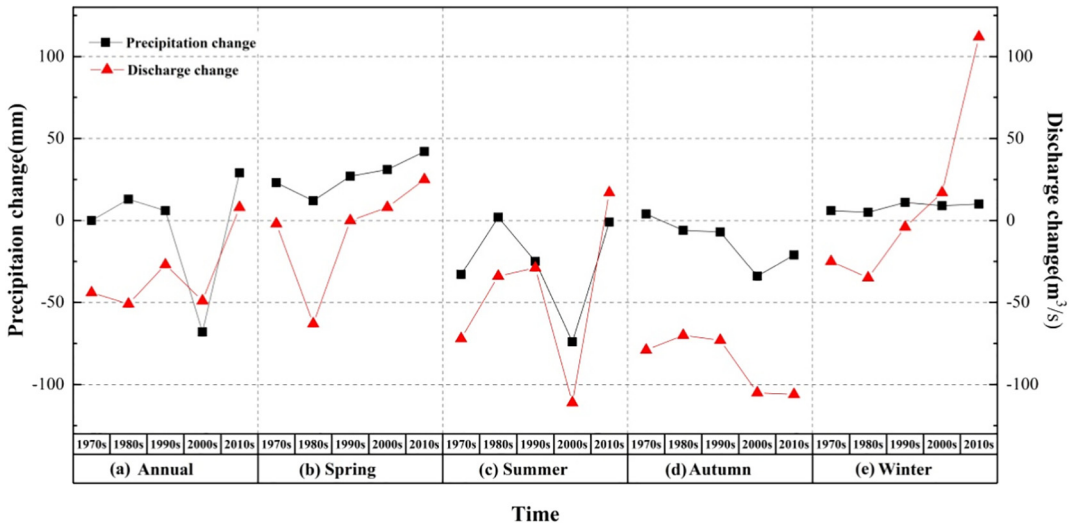

Fig. 11. Decadal variations in annual and season precipitation and discharge.

(3) At the decadal scale, the relative contribution of climate change to discharge changes is positive, except during the 1970s. In contrast, the relative contribution of human activities on discharge changes is negative throughout the entire change period. This was mainly due to the increase of the total population size of the UMR over the past 52 years, which resulted in the increase of water consumption. The cumulative effect of multistage reservoirs led to the increased occurrence of river dehydration, which indirectly resulted in the reduction of discharge. The changes of cultivated land, grassland and forest area largely affected the magnitude of irrigation and evaporation, resulting in reduced discharge. At the seasonal scale, the spatial and temporal distributions of water resources were changed due to the construction of a large number of reservoirs, which stored water in summer and used water in winter. This caused the time which the maximum and minimum discharge occurred to shift. The UMR is a fragile environmental zone (natural disasters, such as earthquakes, floods and debris flow, occur frequently). Therefore, quantifying the relative contributions of climate change and human activities to discharge changes at different temporal scales in the UMR basin is beneficial for reducing the risk of disaster, reasonably allocating water resources, and supporting the decisions of water resource

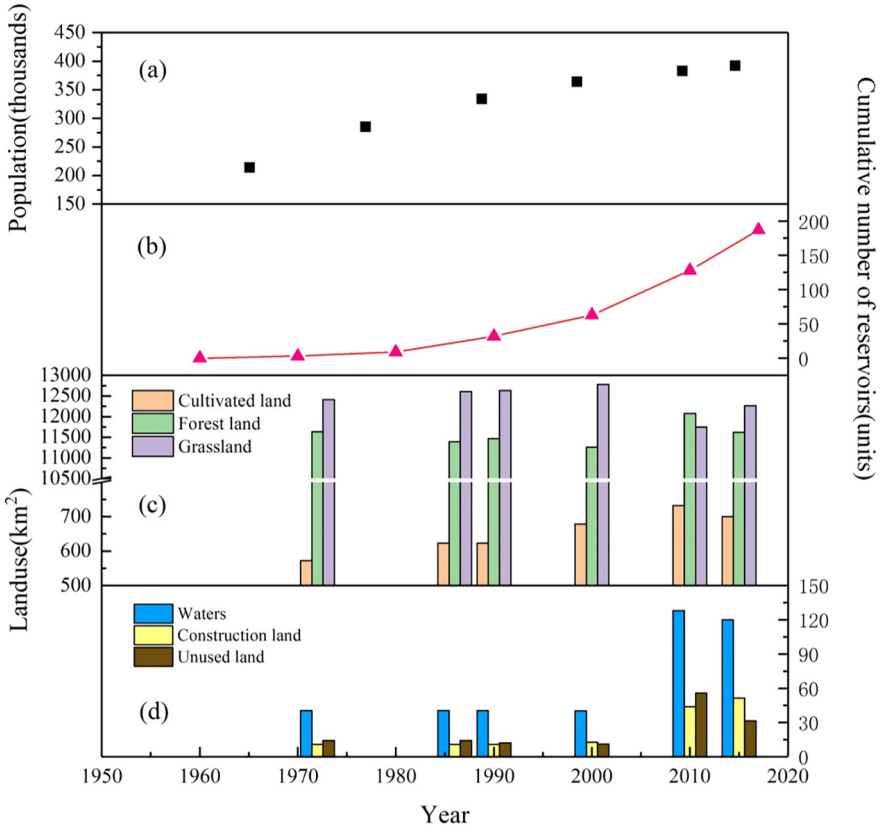

Fig. 12. Changes in population (a), cumulative number of reservoirs (b), and land use (c, d) in the Upper reaches of the Minjiang River basin from 1961 to 2012.

management. However, it is still difficult to quantify exactly the impact of each factor. The effects of specific human activities on discharge changes require further study.

Acknowledgments

Funding: This work was supported by the Strategic Priority Research Program of the Chinese Academy of Sciences (Nos. XDA19070104, XDA20060401), the Natural Science Foundation of China (No. 41475093), the Intergovernmental Key International S&T Innovation Cooperation Program (No. 2016YFE0102400) and the State Key Laboratory of Earth Surface Processes and Resource Ecology Open Research Program (No. 2017-KF-17).

References

Bao, W., Chen, Q., Liu, Z., 1995. Degradation of mountain ecosystem in the upper reaches of Minjiang River and countermeasures for their rehabilitation and reconstruction. Resources and Environment in the Yangtze Valley. 4(3), pp. 277–282 (In Chinese).

Chang, J., Zhang, H., Wang, Y., Zhu, Y., 2016. Assessing the impact of climate variability and human activities on streamflow variation. Hydrol. Earth Syst. Sci. Discuss. 12 (6), 5251–5291.

Gao, P., Mu, X., Wang, F., Li, R., 2010. Changes in streamflow and sediment discharge and the response to human activities in the middle reaches of the Yellow River. Hydrol. Earth Syst. Sci. Discuss. 7 (5), 347–350.

He, Y., Lin, K., Chen, X., 2013. Effect of land use and climate change on runoff in the Dongjiang Basin of South China. Math. Probl. Eng. 2013, 14.

Hu, S., Liu, C., Zheng, H., Wang, Z., et al., 2012. Assessing the impacts of climate variability and human activities on streamflow in the water source area of Baiyangdian Lake. J. Geogr. Sci. 22 (5), 895–905.

Huntington, T.G., 2006. Evidence for intensification of the global water cycle: review and synthesis. J. Hydrol. 319 (1), 83–95.

Kendall, M.G., 1948. Rank Correlation Methods. Griffin, London.

Li, M., 2014. Cumulative Influence of Cascade Hydropower Development on Runoff in Upper Reaches of Minjiang River. Chengdu University of Technology.

Li, A., Zhou, W., Jiang, X., 2005. The graphical information analysis of spatial pattern change of land use/cover during lately years in upper reaches of Minjiang River. J. Mt. Sci. 23 (2), 241–247 (DOI:1008-2786(2005)02-241-07).

Li, Q., Yu, X., Xin, Z., Sun, Y., 2013. Modeling the effects of climate change and human activities on the hydrological processes in a semiarid watershed of loess plateau. J. Hydrol. Eng. 18 (4):401–412. https://doi.org/10.1061/(ASCE)HE.1943-5584.0000629.

Li, Y., Chang, J., Wang, Y., Jin, W., et al., 2016. Spatiotemporal impacts of climate, land cover change and direct human activities on runoff variations in the Wei River Basin, China. WaterSA 8 (6):220. https://doi.org/10.3390/w8060220.

Li, B., Li, C., Liu, J., Zhang, Q., et al., 2017. Decreased discharge in the Yellow River Basin, China: climate change or human-induced? WaterSA 9 (2):116. https://doi.org/10.3390/w9020116.

Luo, P., APIP, He, B., Duan, W., et al., 2015a. Impact assessment of rainfall scenarios and land-use change on hydrologic response using synthetic Area IDF curves. Journal of Flood Risk Management 11:S84–S97. https://doi.org/10.1111/jfr3.12164.

Luo, P., He, B., Takara, K., Xiong, Y., et al., 2015b. Historical assessment of Chinese and Japanese flood management policies and implications for managing future floods. Environ. Sci. Pol. 48:265–277. https://doi.org/10.1016/j.envsci.2014.12.015.

Ma, F., Ye, A., Gong, W., Mao, Y., et al., 2014. An estimate of human and natural contributions to flood changes of the Huai River. Glob. Planet. Chang. 119 (4), 39–50.

Mann, H.B., 1945. Nonparametric test against trend. Econometrica 13 (3), 245–259.

Milliman, J.D., Farnsworth, K.L., Jones, P.D., Xu, K.H., et al., 2008. Climatic and anthropogenic factors affecting river discharge to the global ocean, 1951–2000. Glob. Global & Planetary Chang. 62 (3–4), 187–194.

Milly, P.C.D., Dunne, K.A., Vecchia, A.V., 2005. Global pattern of trends in streamflow and water availability in a changing climate. Nature 438:347–350. https://doi.org/10.1038/nature04312.

Mitchell, J.M., Dzerdzeevskii, B., Flohn, H., et al., 1966. Climate Change. WMO Publ.

Mu, X.M., Zhang, X.Q., Gao, P., Wang, F., 2010. Theory of double mass curves and its applications in hydrology and meteorology. Journal of China Hydrology 30 (4), 47–51.

Pushpalatha, R., Perrin, C., Moine, N.L., Andréassian, V., 2012. A review of efficiency criteria suitable for evaluating low-flow simulations. J. Hydrol. 420–421, 171–182.

Song, X.M., Zhang, J.Y., Zhang, C.S., Liu, C.Z., 2013. Review for impacts of climate change and human activities on water cycle. J. Hydraul. Eng. 44 (7), 779–790.

Sterling, S.M., Ducharne, A., Polcher, J., 2013. The impact of global land-cover change on the terrestrial water cycle. Nat. Clim. Chang. 3 (4), 385–390.

Tan, Q., 2016. Land use type evolution research in the upper reaches of Minjiang River based on GIS and RS. Sichuan Normal University.

Wang, X., 2014. Advances in separating effects of climate variability and human activity on stream discharge: an overview. Adv. Water Resour. 71, 209–218.

Wang, G.S., Xia, J., Tan, G., Lv, A.F., 2002. A research on distributed time variant gain model: a case study on Chaohe River Basin. Prog. Geogr. 21 (6), 573–582 in Chinese. (DOI:1007-6301(2002)06-0573-10).

Wang, D., Hagen, S.C., Alizad, K., 2013. Climate change impact and uncertainty analysis of extreme rainfall events in the Apalachicola River basin, Florida. J. Hydrol. 480 (4), 125–135.

Wei, X., Zhang, M., 2010. Quantifying streamflow change caused by forest disturbance at a large spatial scale: a single watershed study. Water Resour. Res. 46 (12):439–445. https://doi.org/10.1029/2010WR009250.

Xia, J., 1991. Identification of a constrained nonlinear hydrological system described by Volterra Functional Series. Water Resources & Power. 27(9), pp. 2415–2420.

Xia, J., Wang, G.S., Lv, A.F., Tan, G., 2003. A research on distributed time variant gain modeling. Acta Geograph. Sin. 58 (5), 789–796 (In Chinese).

Yang, P., Huang, X., Chai, X., Zhao, J., 2014. Analysis and Prediction of Variation Tendency of Precipitation and Runoff at Dujiangyan Section, MinRiver Catchment. 3. Northwest Hydropower, pp. 1–4 (DOI:1006-2610(2014)03-0001-04).

Ye, A., Xia, J., Wang, G., 2006. Dynamic network-based distributed kinematic wave affluent model. Yellow River. 28(2) :pp. 26–29 in Chinese. 1000-1379(2006)02-0026-03.

Ye, A., Duan, Q., Zeng, H., Li, L., et al., 2010. A distributed time—variant gain hydrological model based on remote sensing. Journal of Resources and Ecology. 1 (3):222–230. https://doi.org/10.3969/j.issn.1674-764x.2010.03.005.

Ye, A., Duan, Q., Zhan, C., Liu, Z., et al., 2013. Improving kinematic wave routing scheme in Community Land Model. Hydrol. Res. 44 (5):886–903. https://doi.org/10.2166/nh.2012.145.

Ye, A., Duan, Q., Schaake, J., Xu, J., Deng, X., Di, Z., Miao, C., Gong, W., 2015. Post-processing of ensemble low flow forecasts. Hydrol. Process. 29:2438–2453. https://doi.org/10.1002/hyp.10374.

Yuan, Y., Zhang, C., Zeng, G., Liang, J., et al., 2016. Quantitative assessment of the contribution of climate variability and human activity to streamflow alteration in Dongting Lake, China. Hydrol. Process. 30 (12):1929–1939. https://doi.org/10.1002/hyp.10768.

Yue, S., Pilon, P., Phinney, B., Cavadias, G., 2002. The influence of autocorrelation on the ability to detect trend in hydrological series. Hydrol. Process. 16 (9):1807–1829. https://doi.org/10.1002/hyp.1095.

Zhang, Z., 1992. Dry valleys in the Hengduan Mountains. Science Press, Beijing.

Zhang, Q., Singh, V.P., Sun, P., Chen, X., et al., 2011a. Precipitation and discharge changes in China: changing patterns, causes and implications. J. Hydrol. 410 (3–4), 204–216.

Zhang, Q., Zhou, Y., Singh, V.P., Chen, X., 2011b. The influence of dam and lakes on the Yangtze River streamflow: long-range correlation and complexity analyses. Hydrological Processes. Hydrol.Process 26 (3):436–444. https://doi.org/10.1002/hyp.8148.

Zhang, M., Wei, X., Sun, P., Liu, S., 2012. The effect of forest harvesting and climatic variability on runoff in a large watershed: the case study in the Upper Minjiang River of Yangtze River basin. J. Hydrol. 464-465(, 13), 1–11.

Zhang, Q., Liu, J., Singh, V.P., Gu, X., et al., 2016. Evaluation of impacts of climate change and human activities on discharge in the Poyang Lake basin, China. Hydrol. Process. 30 (14):2562–2576. https://doi.org/10.1002/hyp.10814.

Zhao, G., Tian, P., Mu, X.M., Jiao, Y., et al., 2014. Quantifying the impact of climate variability and human activities on discharge in the middle reaches of the Yellow River basin, China. J. Hydrol. 519 (PA), 387–398.